

Institute of Physics of the Academy of Sciences of the Czech Republic, v.v.i.,
Division of Solid State Physics, Cukrovarnická str. 10, CZ-16200 Praha;

University of West Bohemia, Univerzitní str. 8, CZ-30614 Plzeň,
Research Centre - New Technologies in Westbohemian Region;

University of Pardubice,
Faculty of Chemical Technology, Studentská str. 573, CZ-53210 Pardubice.



Some Thermodynamic, Structural and Behavioral Aspects of Materials Accentuating Non-crystalline States

Edited by

Jaroslav Šesták

Miroslav Holeček

Jiří Málek



Institute
of Physics



NEW TECHNOLOGIES
RESEARCH CENTRE
UNIVERSITY
OF WEST BOHEMIA



Univerzita
Pardubice

OPS Nymburk 2009 Plzeň ZČU



13. ON THE APPLICATION OF DTA/DSC METHODS FOR THE STUDY OF GLASS CRYSTALLIZATION KINETICS

Vladimir M. Fokin, Aluisio Cabral Jr., Marcio L.F. Nascimento,
Edgar D. Zanotto, Jaroslav Šesták

13.1. Traditional determination of overall crystallization kinetics by thermal analysis

Thermoanalytical (TA) data, such as those determined by differential thermal analysis (DTA) and differential scanning calorimetry (DSC), are of macroscopic nature since the measured overall (observed) occurrence is commonly averaged over both the whole DTA/DSC peak and the sample assemblage under study [1-3]. Despite this fact, experimentally resolved shapes of TA curves have been widely used as a potential source for kinetic appreciation of solid-state reactions taking place in the sample (either internally or superficial) aiming to discriminate stepwise processes of nucleation and crystallization. The shape of a TA curve is often taken as a characteristic feature of the reaction dynamics and its kinetic interpretation is then mathematically linked with the analytical form of model functions, $f(\alpha)$, representing the overall reaction mechanism, which are a part of the traditional relationship:

$$d\alpha / dt = \alpha' = k(T) f(\alpha), \quad (1)$$

where α is the volume fraction transformed at time t (or, for the case focused here the degree of crystallization) derived from the ratios of instantaneous and total areas encircled by a DTA/DSC crystallization peak.

Determination of the so called kinetic constants, such as the value of activation energy, E (inherent in the Arrhenius equation $k(T) = A \exp(-E/RT)$) is typically carried out in two reasonable ways, either to find directly a linear dependence between the functions involved, or by undertaking further differentiation or integration. A rather popular method of kinetic data analysis is based on expressing the maximum values on the dependence of α' vs. T [1,2], which are often displayed as the Kissinger plot [4] (known since 1959) and which, in various modifications [5], is applicable for a series of peak apexes at different heating rates [4-8] using the following expression:

$$\ln(\phi / T_m^2) = \frac{E}{R} \left(\frac{1}{T_m} \right), \quad (2)$$

where ϕ is the heating rate and T_m is the peak (apex) temperature. Worth noting is the similar determination of activation energy for the structural relaxation [9] and viscous flow in the glass structure region from the heating rate dependence of the glass transition temperature T_g or the cooling rate dependence of the limiting fictive temperature T_f using DTA/DSC traces [10].

Recently the so-called integral methods of evaluation became more widespread. They are based on a modified, integrated form of the function $f(\alpha)$, which is determined as

$$g(\alpha) = \int_{\alpha_0}^{\alpha} d\alpha / f(\alpha) = \int_{T_0}^T k(T) dT / \phi. \quad (3)$$

However, it should be emphasized that such a procedure involves the integration of the Arrhenius function $k(T)$, which needs approximations [11], but which sufficiently precise calculation might be seen as a marginal problem, though it has led to exceptionally intense publication activity. It can be shown that its nature leads to simple solutions, because in most kinetic calculations the effect of the approximations is small and is thus routinely neglected, implying that $k(T)$ is considered to behave as an isothermal constant, again, and instead of a complex integration, is simply put in front of the integral ($\int k(T) dt \approx k(T) \int dt$), which is often hidden behind complicated mathematics [1-3,11]. It is worth noting that the plain passage between integral and differential representation must be reversible under all circumstances, though we may recollect early brainteaser of what is the true meaning of partial derivatives of a time-temperature dependent expression of degree of conversion, $\alpha = \alpha(t, T)$ [1,3], which was even misrepresented in former kinetic analysis of glass crystallization [12,13].

The most intricate process is the resolution of a model function, $f(\alpha)$ [1-3] which is not known *a priori* and which is supposed to be determined in analytical form (simultaneously taking into account its plausible diagnostic potential). The specification of $f(\alpha)$ is thus required by means of substitution by an explicit or approximate analytical function frequently derived on basis of modeling the reaction pathways (mechanism) by means of physical-geometric assumptions [14]. Such models usually incorporate a rather hypothetical description of consequent and/or concurrent processes of the interface chemical reaction, nucleation, crystal growth and diffusion structured within the perception of simplified geometrical bodies being responsible for the built-in particles. Such a derived analytical function, $f(\alpha)$, determinedly depends on these physical-chemical and geometrical relations at the interface between the product and the reactants [3,15,16]. Let us remind that if we are not accounting on these interfaces or other inhomogeneity we deal with an apparently uncomplicated case of concentration-dependent homogeneous reactions and $f(\alpha)$ is associated with the so-called reaction order, $(1-\alpha)^n$ [1,3]. However, for glass crystallization the heterogeneity effects ought to be included, which is actually accounting the crystallite interfaces as an explicit disturbing 'defect'. The mathematical description becomes thus more complicated due to the fact that not the (rather undeterminable) bulk concentration but the inherent phase interfaces may carry out the most significant function in controlling the reaction progress. The most common models are derived for isothermal conditions and are often associated with the so called shrinking-core mechanism, which maintains a sharp reaction boundary [3,15,16]. Using a simple geometrical representation, the reacting system can be classified as a set of spheres where the reaction interface must be reached by reacting components through diffusion. Any interfacial (separating) layer bears the role of kinetic impedance and the slower of the two principal processes, diffusion and chemical interface reaction, then become the rate-controlling process.

Isothermal crystallization kinetics is traditionally evaluated using the generalized Johnson-Mehl-Avrami-Yerofeyev-Kolmogorov (JMAKY) equation [17-20], which is accepted as the rate equation for all types of interface-controlled crystallization, as well as for the case of diffusion-controlled crystallization [1-3,21] in the comprehensive form of

$$\ln(1-\alpha) = -(k(T)t)^r \quad (4)$$

Generally the exponent, r , can be seen as a multipart number as a robust analysis of the basic JMAYK equation reveals that the apparent (overall) values of activation energies, E_{app} (particularly being the center of interest when determined on the basis of DTA/DSC measurements), can be commonly correlated to the partial activation energies of nucleation, E_N , growth, E_G and/or diffusion, E_D . It follows that

$$E_{app} = \frac{aE_N + bdE_G}{a + b + d}, \quad (5)$$

where a and b are characteristic multiplying constants providing that the denominator ($a + b + d$) equals to the power exponent, r , of the JMAYK equation, and the value b corresponds to 1 or $\frac{1}{2}$ related to the movement of growth front controlled by either chemical reaction (1) or diffusion ($\frac{1}{2}$). Moreover, the coefficients d and b are associated with the nucleation velocity and the growth dimension, respectively; see Table 1 [22].

Table 1. DIMENSIONALITY OF NUCLEATION AND GROWTH

nuclei↓ growth⇒	Growth dimension	Interface reaction $E_{app} =$	Diffusion controlled $E_{app} =$
Instantaneous nucleation from fixed sites	1-D	$r=1, E_G$	$r=0.5, E_D/2$
	2-D	$r=2, 2 E_G$	$r=1, E_D$
	3-D	$r=3, 3 E_G$	$r=1.5, 2 E_D/3$
Constant rate of homogeneous nucleation	1-D	$r=2, E_G + E_N$	$r=1.5, E_D/2 + E_N$
	2-D	$r=3, 2 E_G + E_N$	$r=2, E_D + E_N$
	3-D	$r=4, 3 E_G + E_N$	$r=3, 3 E_D/2 + E_N$

This mathematical treatment can be extended to other thermal regimes (such as a non-isothermal, which is common during DTA/DSC measurements) by incorporating a temperature-dependent integration [23-26]. Such a case was analyzed in detail by Kemeny and Šesták [27] yielding the concealed but anticipated fact that the non-isothermal equivalent of the isothermally derived JMAYK differs only by an integration-dependent, dimensionless multiplying constant [1-3,11]. However, the JMAYK relation bears its analytical integral form, too, i.e.,

$$g(\alpha) = (1 - \alpha)[- \ln(1 - \alpha)]^p, \quad (6)$$

which is sometimes generalized into a two exponent (JMAYK modified) equation,

$$g(\alpha) = (1 - \alpha)^n [- \ln(1 - \alpha)]^p \cong (1 - \alpha)^n \alpha^m, \quad (7)$$

where p is related to the original form of JMAYK through the relation $p = (1 - 1/r)$. In practice, however, the introduction of new exponent n may result that both values of n and p may become numerically non-integral. The JMAYK equations (6) and (7) have been widely applied for the description of overall crystallization kinetics yielding numerous data on "apparent" activation energies and power exponents. When allowing for the existence of fractal exponents, there is almost no restriction to its matching

applicability, however, a simple preliminary test of the JMAYK applicability to a given type of DTA/DSC peak may be useful on basis of its asymmetry [28] and worth of application before actual kinetic analysis. The shape of continuous-heating DSC/DTA peak, which is supposed to be compatible with the JMAYK equation, is routinely asymmetrical (somewhat irrespectively to the power exponents) but the peaks always exhibit shifts of their apexes with increasing heating rate showing slower rise on its low-temperature (onset) side [29, 30]. Such a peak asymmetry is a characteristic feature for the majority of simple interface and/or diffusion controlled crystallizations. Any temperature pre-annealing usually increases its initially transformed fraction, which shifts the peak to lower temperatures and makes it broaden.

Worth mentioning is another relevant alternative to the JMAYK crystallization kinetics, which is the so-called NGG mechanism (normal-grain-growth model) introduced by Atkinson [31], which has been effectively applied by Illekova [32] and at her chapter "Kinetic characteristic of nanocrystal formation in metallic glasses" in [33]. It factually reflects the process of coarsening of the microcrystalline phases, justifiable in most cases of nano-crystalline glass-ceramics (like finemetals) when the mean grain size is below 10 nm. In this instance, the shape of DSC/DTA exothermic peak becomes different with an atypical symmetry (when comparing with JMAYK peaks) with little shifts of the apexes with heating rate. The discrepancy results from rationales arising from the differences in JMAYK and NGG modeling. The process of pre-annealing has also different consequences increasing the initial micro-grain radius, thus shifting the onset of the NGG peak to higher temperatures and leading to a narrower transformation range.

We should mention that the term $[- \ln(1 - \alpha)]^p$ can be mathematically converted to another simpler function, α^m , through an expansion in the infinite series, recombined and converted back. The resulting two parameter form, $\alpha^m(1 - \alpha)^n$, is identical to the Šesták-Berggren (SB) equation [34], which has been widely used throughout kinetic examinations resulting in abundant literature on transformation kinetics [1-3]. This equation consists of two essential but counteracting parts, the first responsible for mortality, $\cong \alpha^m$ (i.e., reagent disappearance and product formation) and the other for fertility, $\cong (1 - \alpha)^n$ (i.e., a kind of product hindrance generally accepted as an 'autocatalytic' effect) resembling an extended reaction-order concept $(1 - \alpha)^n$ (particularly when completed by the so called "accommodation function" α^m [35]). Such a SB equation has, however, no analytical form for its integral version, but is conventionally exploited in those cases where the standard JMAYK equation (6) fails to provide reasonable values of the power exponents losing thus its desired diagnostic role and providing mere data fitting. Nevertheless this SB equation has become a standard method of kinetic evaluation [36] with a wide applicability [37] and, in some cases, used instead JMAYK equation [38-41].

There have been numerous studies on glass crystallization kinetics [2, 42-44], but their foremost trouble is that most kinetic data are assessed only on the basis of TA measurements, which are, in many cases, rather incompatible with visual observations [45]. We found some matching data between a DTA study and electrical measurements of conductivity [46,47] and did a thorough investigation on bulk and powder crystallization of glasses in the system $\text{SiO}_2\text{-Al}_2\text{O}_3\text{-ZnO}$ doped with ZrO_2 [48,49]. DTA measurements were accomplished on glassy samples casted either directly to the DTA cells (diameter 7mm, height 10mm) or additionally powdered. Separate modes of nucleation and crystal growth were examined by optical observation in a microscope.

Good coincidence was found between the onset of DTA peaks with that calculated from optically determined nucleation and growth data. By application of the JMAYK equation, the DTA curve was reconstructed on the basis of the overall degree of crystallization adjusted to the nucleation and growth figures bestowing a rather good coincidence between calculated and measured curves. However, such a type of detailed analysis is often missing in recent studies though it is much needed for reaching a better appreciation of DTA measurements [50,51] and more trustworthy kinetic evaluation. A better elucidation of DTA/DSC measurements is the purpose of our contribution showing some examples in the next paragraphs.

13.2. Determination of crystal nucleation rates from TA methods

About a century ago Gustav Tamman [52] proposed a method to estimate the number density of crystal nuclei in undercooled organic liquids. The technique relies on the development of such nuclei at a relatively high temperature (higher than the previous nucleation temperature) up to a size large enough to be visible with optical or electron microscopy. This method - known as Tamman's or "development" method - has been extensively used to measure crystal nucleation rates in inorganic glasses since 1968 [53, 54]. For a number of silicate glasses, nucleation rates varying from about $10\text{m}^{-3}\text{s}^{-1}$ to $10^{13}\text{m}^{-3}\text{s}^{-1}$ have been estimated by Deubener and Fokin respectively [55]. This method gives correct values of the number of super critical nuclei, needed for estimation of the nucleation rates and the time-lag for nucleation, but is quite laborious and cannot be always employed.

Beginning in 1980s, other methods based on DTA/DSC experiments have been developed [56-61]. These non-isothermal methods are, in principle, faster than the traditional (isothermal) microscopy method and can be divided in two following groups:

i) The first of them the crystal growth rate than on the number of crystals. allows one to determine the temperature dependence of the nucleation rates. To start a study of nucleation kinetics one often needs to know the temperature range covering to the nucleation rate maximum. Such types of non-isothermal methods are based on the reasonable assumption that the inverse temperature of the crystallization peak, $1/T_c$, on a DSC/DTA curve is proportional to the number density of nuclei, since the higher the crystal number the faster is the overall crystallization kinetics and, hence, the release of the heat of crystallization can be detected at a lower temperature. Therefore, a plot of $1/T_c$ versus T_N , the temperature of pre-nucleation heat treatment for a given time may reflect the temperature dependence of the nucleation rate, or more exactly, the crystal number density nucleated in a given period of time. Sometimes, the height of the crystallization peak is used, since, to a first approximation, the peak area is considered constant, but it is noticeable that its width decreases with increasing crystal number. This effect results in an increase of the height of the exothermic peak. It should be noted, however, that the time necessary for full crystallization, which determines the width of the crystallization peak, depends more on

ii) The second method, proposed by Ray and Day [60], is based on a pre-heat treatment of the glass samples to induce partial crystallization and on the estimation of the crystallized volume fraction by the decrease of the crystallization peak area, A , of the residual glass on a DTA/DSC curve. The preliminary nucleation at T_N for time t_N plus growth at $T_G > T_N$ for time t_G lead to a decrease of the fraction of residual glassy matrix. The crystallized volume fraction, α , is given by the above mentioned JMAYK

(Jonhson-Mehl-Avrami-Yerofeeyev-Kolmogorov [17-20]) Eq. (4) adjusted for a more detailed description of growth of a given number of crystals with constant rate U :

$$\alpha(t_c) = 1 - \exp\left(-\frac{4\pi}{3}(I(T_N)t_N + N_{at})U(T_G)t_G^3\right) \quad (8)$$

Here $(I(T_N)t_N + N_{at})$ is the total number of nuclei formed by nucleation at T_N with rate I plus athermic nuclei (N_{at}), which include the nuclei formed during cooling of the melt (quenched-in nuclei, N_q) and during the heating run up to the temperature T_G .

The decrease of the residual glass fraction due to preliminary crystallization reduces the crystallization peak area, A , since, in the general case, it is proportional to the mass of transformed material. Varying the growth time, t_G , at fixed nucleation conditions (T_N, t_N) one can change α and hence A . The following equation was proposed by Ray and Day [60] for the ratio of the peak areas corresponding to different t_G

$$\frac{A_1}{A_2} = \frac{M_1 \left[1 - \frac{4\pi}{3}(I t_N + N_{at})(U t_{G1})^3\right]}{M_2 \left[1 - \frac{4\pi}{3}(I t_N + N_{at})(U t_{G2})^3\right]}, \quad (9)$$

where M_1 and M_2 are the sample mass for two DSC runs corresponding to the time of preliminary growth, t_{G1} and t_{G2} , respectively.

To derive Eq.9 the exponent in Eq.8 was expanded. Hence Eq.9 is limited to $\alpha \sim 0.2-0.3$. By knowing $A_i, M_i, (i=1, 2)$ and $U(T_G)$, via Eq.9 one can estimate N_{at} together with the number of crystals $N = I t_N$ nucleated at T_N . The number of athermic crystals can be estimated separately by the same equation, with the difference that the preliminary crystallization step does not include the nucleation procedure, i.e. $t_N=0$.

Tests of the above described methods have been performed in refs. [60, 61] using literature data for the nucleation and growth kinetics in stoichiometric lithium disilicate, $\text{Li}_2\text{O} \cdot 2\text{SiO}_2$ (L_1S_2) and sodium calcium silicate, $\text{Na}_2\text{O} \cdot 2\text{CaO} \cdot 3\text{SiO}_2$ ($\text{N}_1\text{C}_2\text{S}_3$) glasses revealing volume nucleation. However, the overall crystallization kinetics is very sensitive to the crystal growth rate, which in turn strongly depends on the glass viscosity, and this can be significantly affected by impurities that are often not controlled, e.g. "water". Moreover, to correctly employ the value of growth rate one has to know the shape of the crystals.

The aim of this chapter is thus to describe an experimental test of the main assumptions underlying the above DSC/DTA methods by using glass samples produced from the same melts for both the thermo analyses and direct measurements of crystallization kinetics by optical microscopy (sometimes we analyzed by optical microscopy samples before and after a DSC run). We will give special attention to the ratio between surface and volume crystallization, and also to the presence of quenched in nuclei, since the knowledge of their number is relevant for the estimation of the number density of crystals nucleated at given temperature. We do not perform an extensive analysis; our main purpose is merely show that the use of DSC/DTA techniques for the study of crystallization kinetics demands utmost care, since thermo analysis is an integral method and is not self-reliant.

Following refs. [60, 61], two silicate glasses with stoichiometric compositions $\text{Li}_2\text{O}\cdot 2\text{SiO}_2$ (L_1S_2) and $\text{Na}_2\text{O}\cdot 2\text{CaO}\cdot 3\text{SiO}_2$ ($\text{N}_1\text{C}_2\text{S}_3$) were employed as "model" objects. The glasses were synthesized in a platinum crucibles in an electrical furnace at 1450-1500°C for 2 hours. The chemicals were sodium, lithium, and calcium carbonates of analytical grade and ground Brazilian quartz (>99.99% SiO_2). The chemical analysis of the sodium calcium silicate glass is shown in Table 2.

Table 2.

	Na_2O mol %	CaO mol %	SiO_2 mol %
Nominal	16.67	33.33	50
$\text{N}_1\text{C}_2\text{S}_3$ glass	17.2	32.3	50.5

The temperature of the DSC crystallization peak of the parent L_1S_2 glass, which is highly sensitive to small departures of stoichiometry [62], and the experimental values of the nucleation and growth rates give indirect evidence that its composition is close to stoichiometric lithium disilicate. Thermo analyses were performed in a Netzsch 404 Differential Scanning Calorimeter (DSC) using bulk samples of about 35-38 mg. The Tammann method [55] was employed to directly measure the crystal nucleation rates. The crystal sizes, numbers, and respective volume fractions in properly heat treated glass samples were estimated by a Leica DMRX optical microscope coupled with a Leica DFC490 CCD camera.

13.2.1 Number of crystal nuclei and crystallization peak temperature.

To create different numbers of supercritical nuclei, the glass samples were heat treated for different periods of time at temperatures of appreciable nucleation rate. Then each sample was divided into two pieces: one of them was submitted to a DSC run with heating rate of 10°C/min, and the other was heat treated at a higher temperature to develop the nucleated crystals up to visible sizes in an optical microscope and to estimate its number density by stereological methods. Figs.1 and 2 show the number of crystals versus nucleation time at $T=473$ at 590°C for L_1S_2 and $\text{N}_1\text{C}_2\text{S}_3$ glasses, respectively. The solid lines resulted from fitting the experimental values $N(t)$ to the Colins and Kashchiev equation [63, 64]

$$N(t) = I_{st} \tau \left[\frac{t}{\tau} - \frac{\pi^2}{6} - 2 \sum_m \frac{(-1)^m}{m^2} \exp\left(-m^2 \frac{t}{\tau}\right) \right], \quad (10)$$

where τ is the time-lag for nucleation, which characterizes the time to achieve a steady-state nucleation rate I_{st} . The dotted lines are the asymptote of Eq.(10)

$$N(t) = I_{st} \left(t - \frac{\pi^2}{6} \tau \right) \quad (11)$$

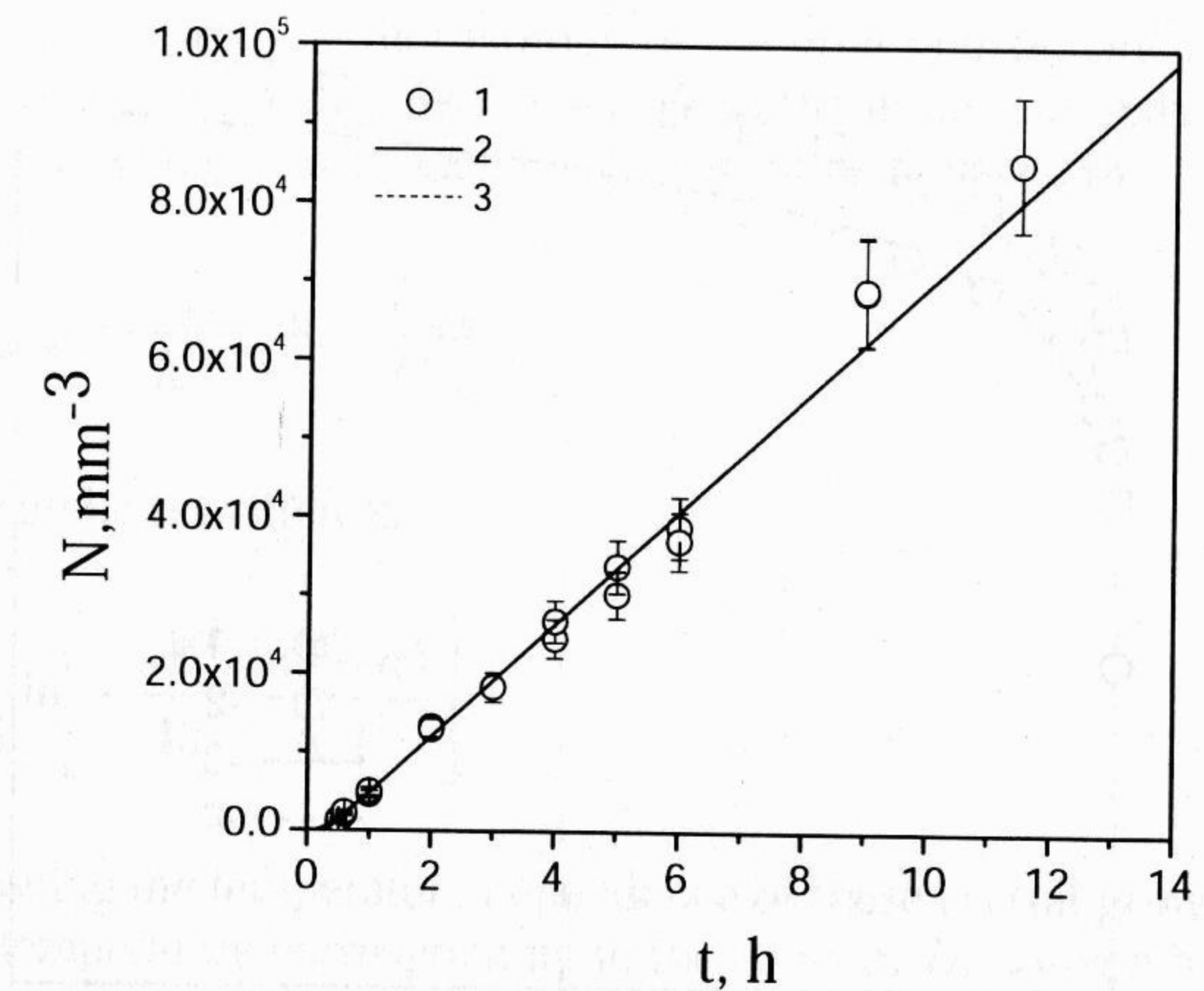


Fig.1 Number density of lithium disilicate crystals versus nucleation time at $T=473^\circ\text{C}$ measured by the development method. The lines 2 and 3 were plotted according to Eqs. 10 and 11, respectively.

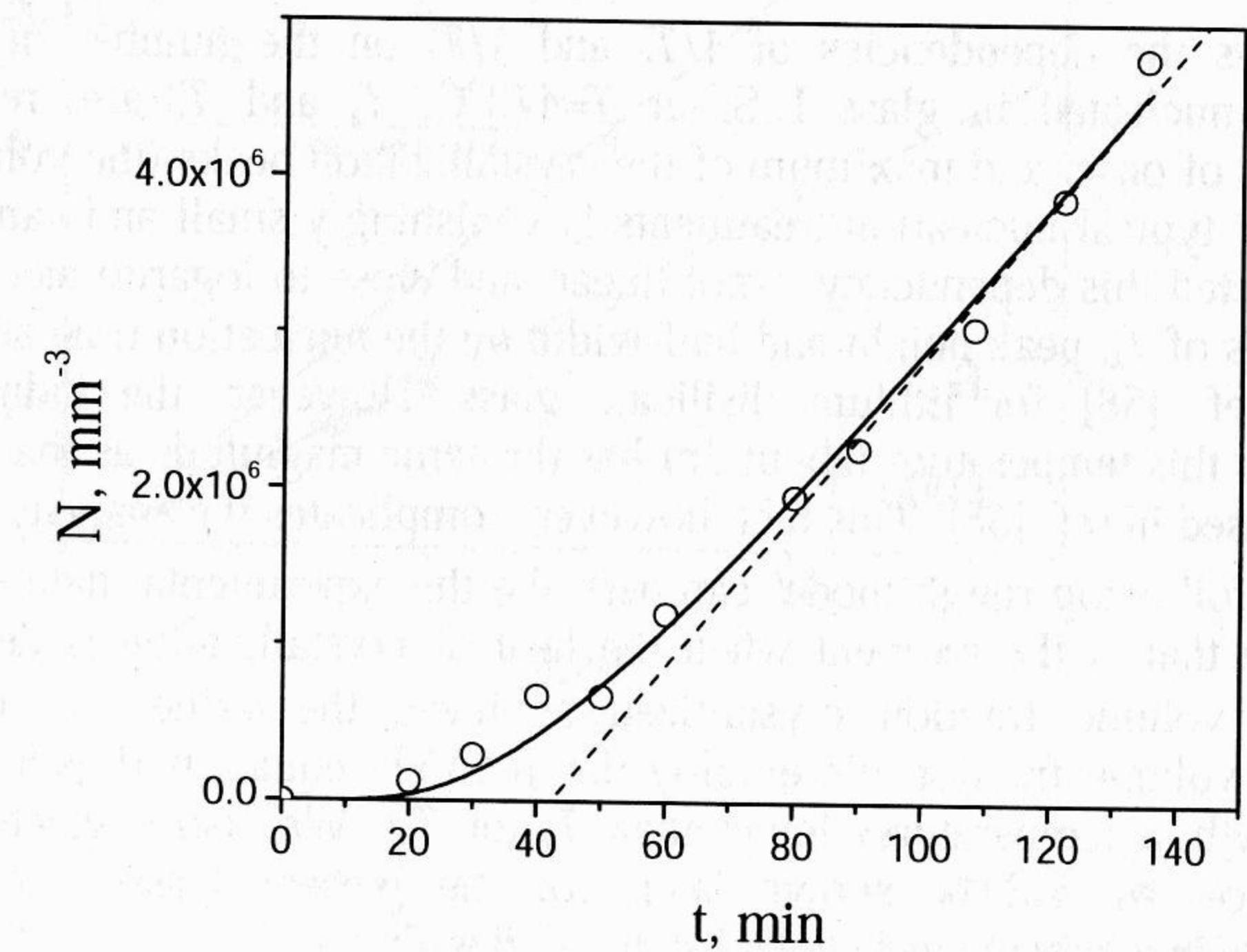


Fig.2. Number density of crystals in $\text{N}_1\text{C}_2\text{S}_3$ glass versus time of nucleation at $T=590^\circ\text{C}$ measured by the development method. The solid and dotted lines were plotted by using Eq.10 and Eq.11, respectively.

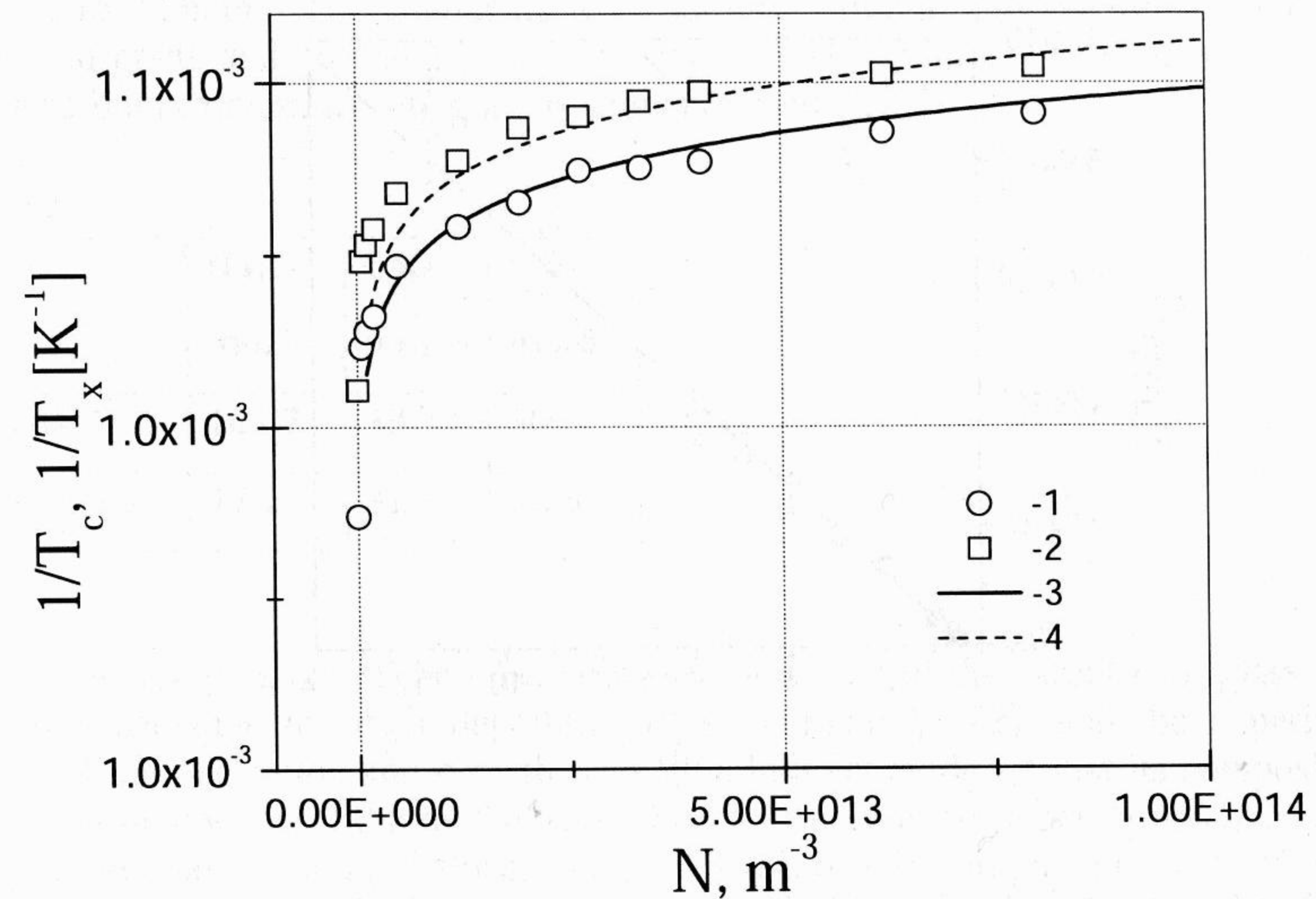


Fig.3. $1/T_c$ (1) and $1/T_x$ (2) versus N for lithium disilicate glass. The lines were fitted to Eq.16, see text.

Fig. 3 shows the dependencies of $1/T_c$ and $1/T_x$ on the number of crystal nuclei preliminary nucleated in glass L_1S_2 at $T=473^\circ\text{C}$. T_x and T_c are, respectively, the temperatures of onset and maximum of the crystallization peaks (the volume fraction of crystals after typical nucleation treatments is vanishingly small and can be neglected). As we expected this dependency is not linear, and close to logarithmic. The non linear dependencies of T_x , peak height and half-width on the nucleation time at $T=453^\circ\text{C}$ were shown in ref. [58] for lithium disilicate glass. However, the induction time for nucleation at this temperature (about 3h) has the same magnitude as the total nucleation time (10h) used in ref. [58]. This fact, however, complicates the analysis of their results.

The following rough model can describe the experimental data shown in Fig.3. We suppose that at the moment when the heat of crystallization is detected by DSC (DTA) the volume fraction crystallized achieved the value α . To estimate the crystallized volume fraction we employ the JMAK equation (Eqs.8, 12) neglecting crystal growth at temperatures lower than T_x (or T_c). We also neglected the athermal crystals since, as will be shown later, for the present glasses and experimental conditions their number is very low as compared with N .

$$\alpha = 1 - \exp\left(-\frac{4\pi}{3} N U^3 t^3\right) \quad (12)$$

We thus believe that this volume fraction α was crystallized via growth with rate $U(T_x)$ in a narrow temperature interval characterized by some effective temperature close to T_x (T_c) of the crystals preliminary nucleated at T_N [$N = I(T_N)t_N$]. Since, in the temperatures of interest, the morphology of the lithium disilicate crystals is close to an ellipsoid of revolution, with growth rates along the minor and major diameters U_{min} and U_{max} , respectively, the growth rate in Eq.12 must be replaced by:

$$U^3 = U_{min}^2 U_{max} = \frac{U_{max}^3}{K^2}; \quad K = \frac{U_{max}}{U_{min}} \quad (13)$$

Then Eq.12 can be rewritten as

$$\ln(U_{max}) = \frac{1}{3} \ln\left[-\frac{3K^2 \ln(1-\alpha)}{4\pi N t^3}\right] \quad (14)$$

Thus, by knowing the temperature dependence of these crystal growth rates, one can estimate the temperature corresponding to the value of U_{max} given by Eq.14.

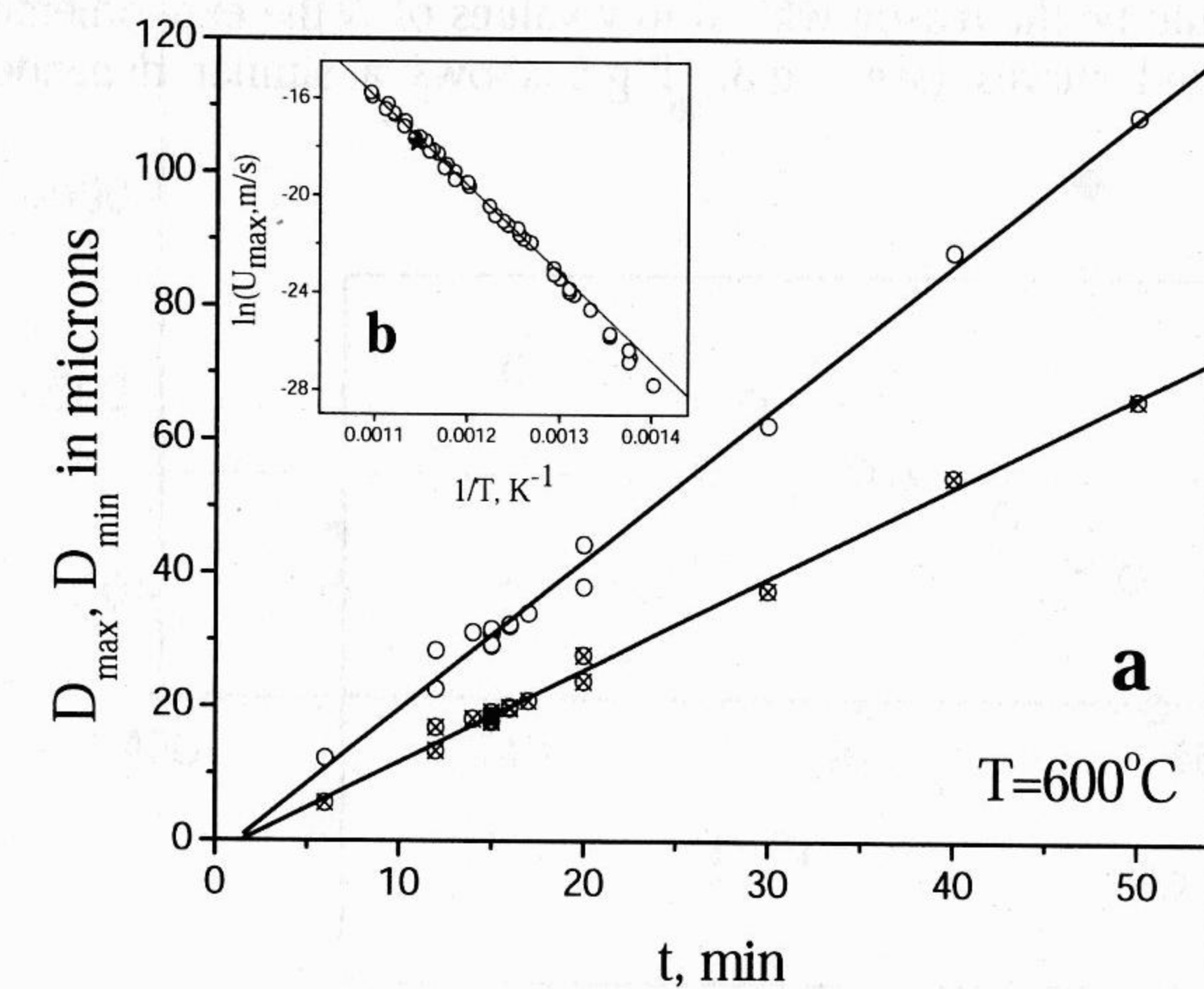


Fig.4. (a) Major and minor crystal axes of lithium disilicate crystals versus time of heat treatment at $T=600^\circ\text{C}$. The lines are linear fits to the experimental points. (b) Arrhenius plot for the crystal growth rate of the major crystal axis [65]. The solid line is a linear fit of the high temperature part of the plot. The black star refers to the data of Fig.4 (a).

Fig.4 shows, as an example, the values of the maximum and minimum diameters of lithium disilicate crystals versus heat treatment time at $T=600^\circ\text{C}$. The inset shows literature data on the temperature dependence of U_{max} for lithium disilicate glass [65] in Arrhenius coordinates. The star corresponding to $T=600^\circ\text{C}$ (our own data for the present

glass) is very close to the other points. At high temperatures $U_{max}(T)$ can be approximated by the following equation (see solid line in Fig.4, inset)

$$\ln(U_{max}, m/s) = 23.79 - 36124.02 \frac{1}{T}; T \text{ in K.} \quad (15)$$

Combining Eqs.(14) and (15), one obtains

$$\frac{1}{T} = \frac{23.79 - \frac{1}{3} \ln \left[\frac{3K^2 \ln(1-\alpha)}{4\pi Nt^3} \right]}{36124.02} \quad (16)$$

Thus Eq.16 gives an inverse effective temperature (at which the volume fraction crystallized arrives at the value α during period of time t) as a function of the number of crystals, N . Curves 3 and 4 on Fig.3 were plotted using Eq.16 for $t=90s$ and $\alpha=0.2$ and 0.1 , respectively. $C=10^\circ\text{C}/\text{min}$ with $t=90s$ corresponds to a temperature interval of 15°C . Despite the rough approximations, this model with reasonable parameters gives a satisfactory qualitative description of the experimental data. It should be noted that the model does not take surface crystallization into account (that is most important for low values of N). May be this would be the reason why at low values of N the experimental points are above the calculated curves (see Fig.3). Fig.5 shows a similar dependence for $N_1C_2S_3$ glass

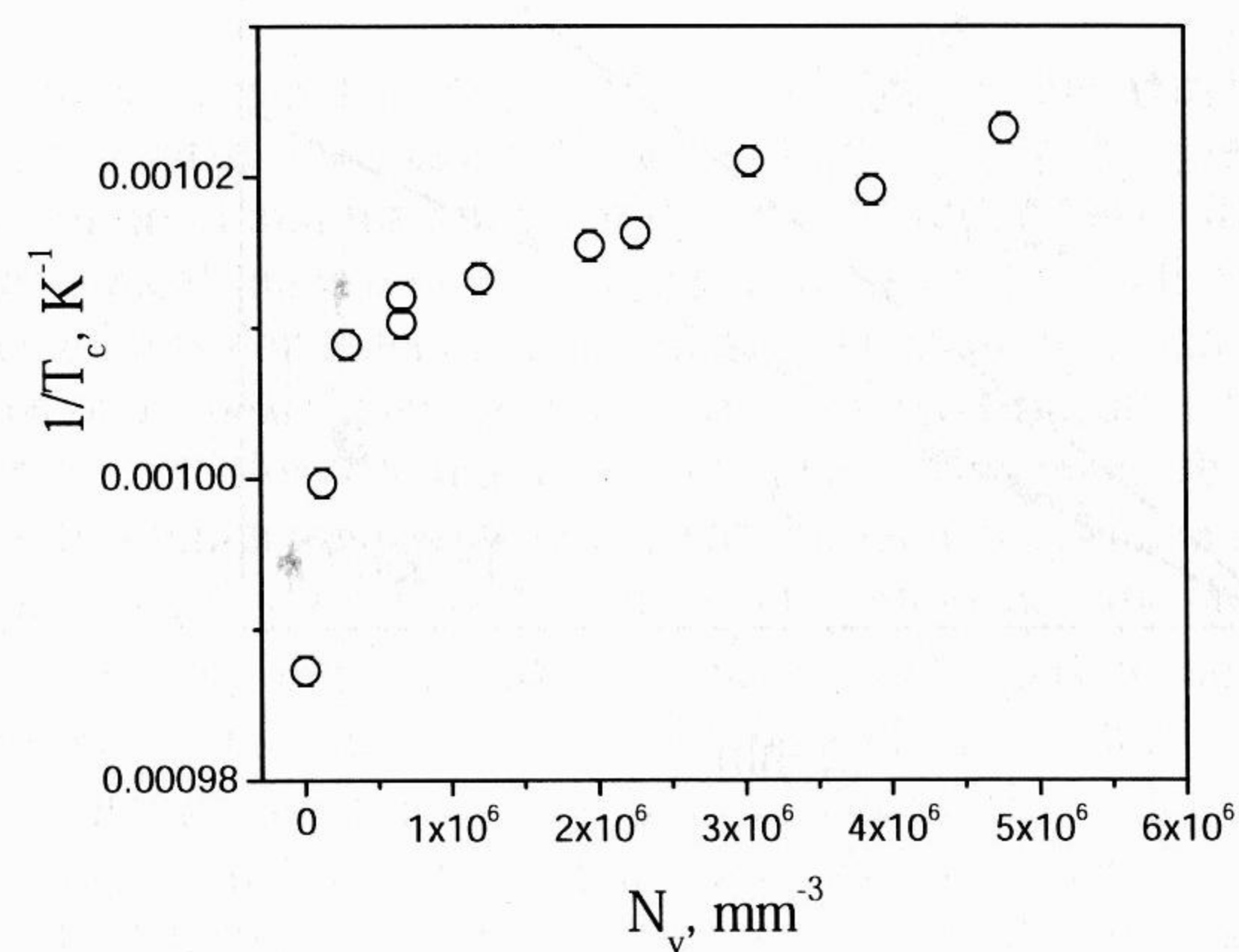


Fig.5 $1/T_c$ versus N for a stoichiometric soda-lime-silica glass, $N_1C_2S_3$.

The following comments on the method employing the shift of the crystallization peak position to estimate nucleation rate curve should be done:

- (i). This method gives an accurate temperature dependence of the nucleation rate only if non-steady nucleation can be neglected, i.e. the equality $N(T_N) = I_{st}(T_N)t_N$ holds, where I_{st} is the steady-state nucleation rate. This is

the case of relative high temperatures or long heat treatment time t_N that significantly exceeds the time-lag for nucleation at all studied temperatures. In all other cases the method will distort the temperature dependence of the nucleation rate at low temperatures (especially close to or below the glass transition temperature). As an illustration, Fig.6 shows the number of lithium disilicate crystals versus nucleation temperature for a fixed nucleation time $t=3h$ (same time used in ref. [58]) together with the number of crystals which should be nucleated during the same period of time if steady-state nucleation had been achieved. Fig.7 shows similar plots for $N_1C_2S_3$ glass. It is clear that due to the time-lag for nucleation the above method has to lead to a significant decrease of the temperature interval of detectable nucleation rate for L_1S_2 glass, and only to a weak one for $N_1C_2S_3$ glass which at given temperatures has a time-lag lower than that in lithium disilicate glass. However, it is difficult to take into account the effect of time-lag if nucleation data is not preliminary available.

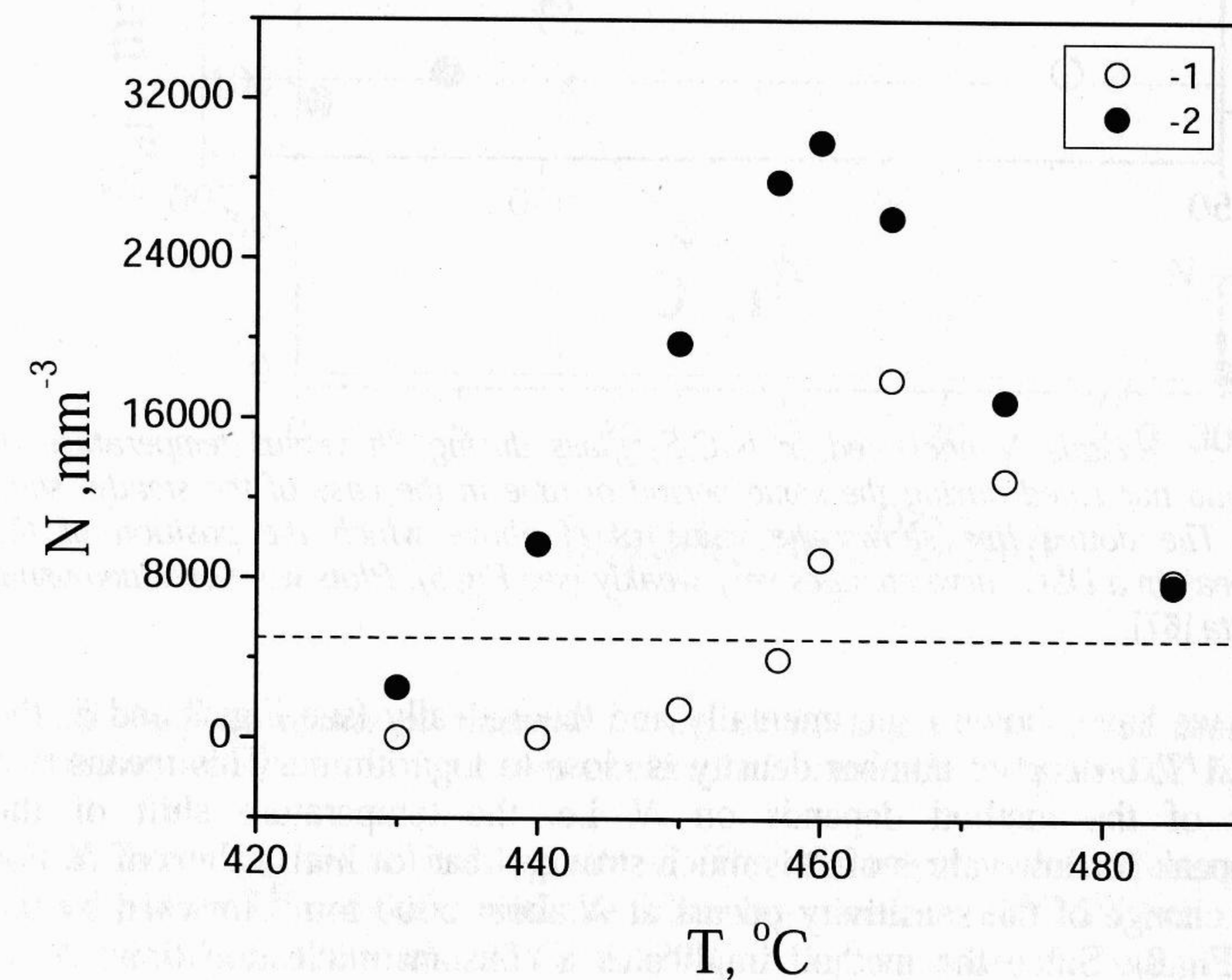


Fig.6. Number of lithium disilicate crystals N nucleated during 3h versus nucleation temperature (1) and nucleated during the same period of time in the case of the steady-state nucleation (2). The dotted line shows the value of N above which the position of the crystallization peak in a DSC curve changes very weakly (see Fig.4). Plots were obtained using experimental data [66].

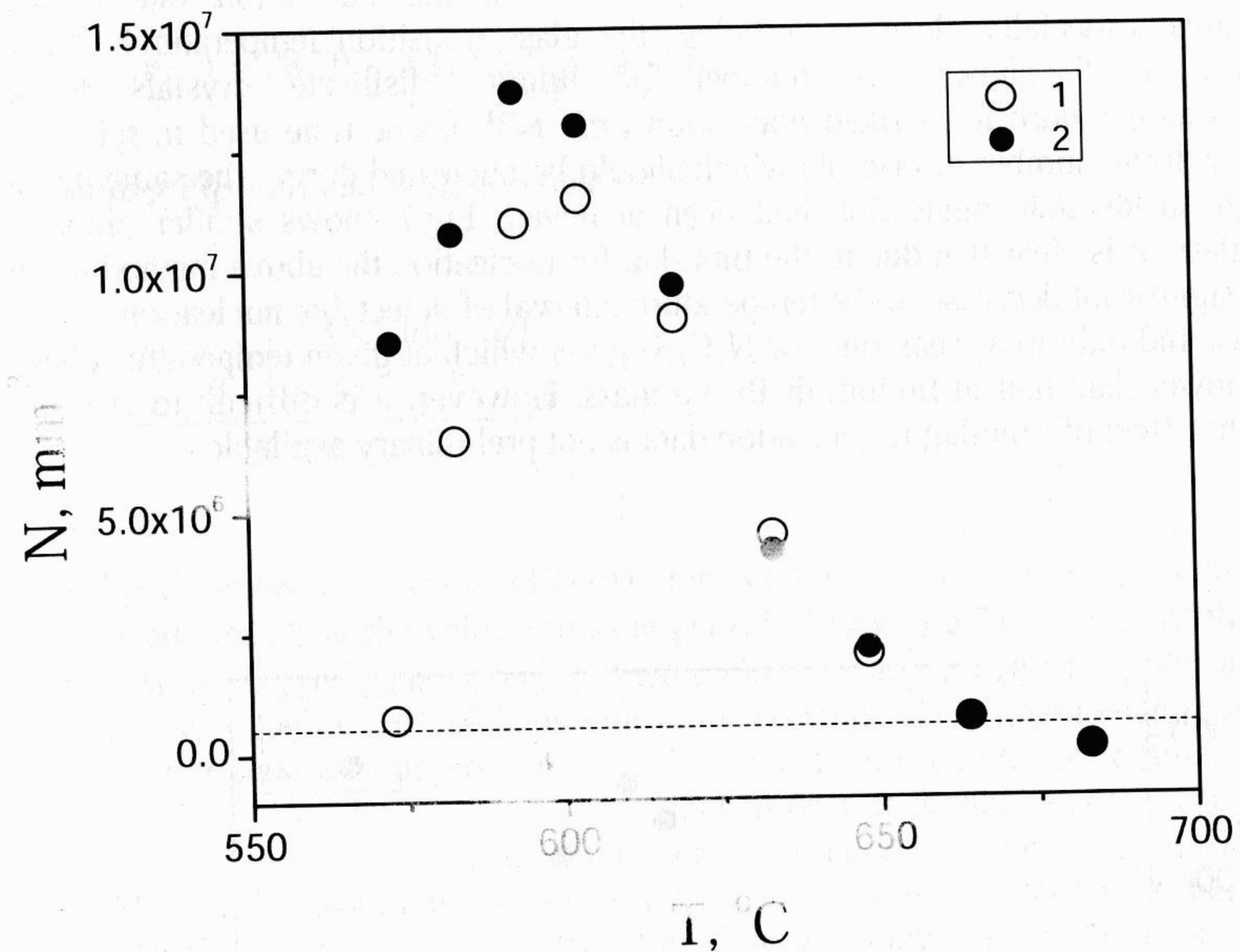


Fig.7. Number of crystals N nucleated in $N_1C_2S_3$ glass during 3h versus temperature of nucleation (1) and nucleated during the same period of time in the case of the steady-state nucleation (2). The dotted line shows the value of N above which the position of the crystallization peak in a DSC curve changes very weakly (see Fig.5). Plots were obtained using experimental data [67].

(ii). As we have shown experimentally and theoretically (see Figs.3 and 5) the dependence of $1/T_c$ on crystal number density is close to logarithmic. This means that the sensitivity of the method depends on N , i.e. the temperature shift of the crystallization peak for low values of N is much stronger than for high values of N . For L_1S_2 glass the change of the sensitivity occurs at N about 5000 mm^{-3} (marked by the dotted line in Fig.6). Since the method implicates a constant nucleation time, t_N , N depends on the temperature of nucleation (see Figs.6 and 7). Hence, if the values of $N(T_N)$ belong to different parts of the $1/T_c$ vs N plot, the shift of the crystallization peak temperature would be stronger for temperatures below and above the maximum nucleation rate than that corresponding to the temperatures of maximum. This is the case of L_1S_2 glass (Fig.6), while for $N_1C_2S_3$ glass all values of $N(T_N)$ belong to the same part of $1/T_c$ vs N plot (see Fig.7). Thus the logarithmic dependence of $1/T_c$ on N can forge the shape of the temperature dependence of the nucleation rate. Hence, similarly to the case discussed in the previous paragraph, to take into account the non linear dependence of $1/T_c$ on N some nucleation data for the glass understudied are required.

13.2.2. Quench-in and athermal nuclei

As we have shown in the first paragraph, the method to estimate the number of nucleated crystals elaborated by Ray, Fang and Day [60] yields the total number of

nuclei (not only formed at the given nucleation temperature $N(T_N)$, but also the nuclei nucleated at non isothermic (and not always controlled) regime denoted athermal nuclei, N_{at}). To estimate N_{at} independently on the method suggested in ref. [60], we simulated DSC runs with different heating rates in an electrical furnace. Samples of L_1S_2 glass were dropped into a vertical furnace at $T=400^\circ\text{C}$, heated with a rate C up to $T_C=600^\circ\text{C}$, and then treated at this temperature for 40 min to allow crystal growth up to a microscope detectable size.

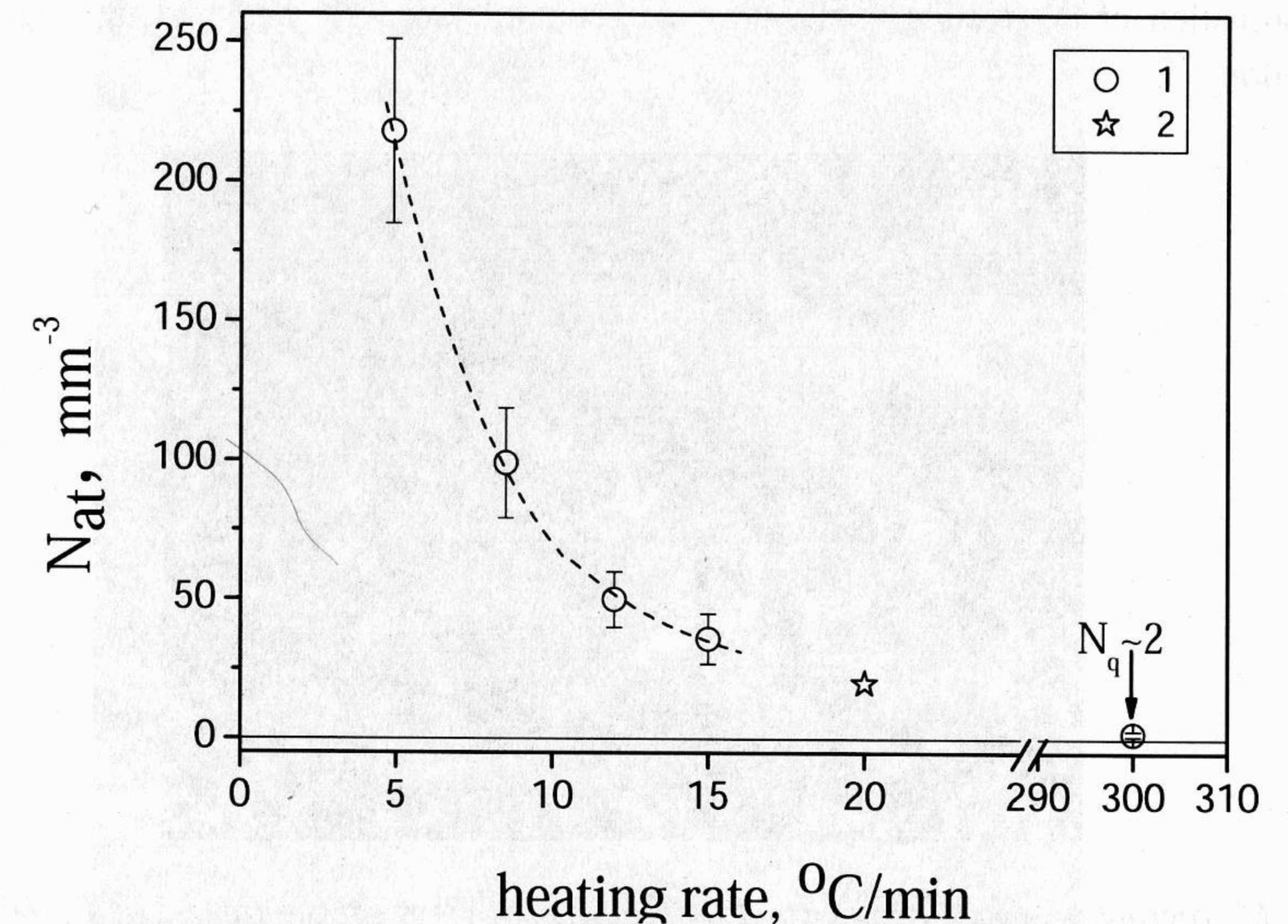


Fig.8. Number density of athermal lithium disilicate crystals versus heating rate. Heat treatments were performed in a vertical electrical furnace (1) and in the DSC furnace (2).

Fig.8 shows N_{at} versus heating rate C . The star refers to heat treatments performed directly in the DSC furnace with the following schedule: $20^\circ\text{C}-5^\circ\text{C}/\text{min}-40^\circ\text{C}$ (5 min) - $20^\circ\text{C}/\text{min}-620^\circ\text{C}$ (20 min) - $20^\circ\text{C}/\text{min}-20^\circ\text{C}$. A higher value of C was realized when the samples dropped into the furnace preliminary stabilized at $T_C=600^\circ\text{C}$. A photo of this sample is shown in Fig.9.

As one can see, the dependence of N_{at} on C is not linear, as could be expected in the case of steady-state nucleation. The effect of non steady-state nucleation is more pronounced at high values of C . In this case the time spent by the sample during the passage through the temperature range corresponding to the non steady-state nucleation is lower than the induction period for nucleation.

One can distinguish two kinds of lithium disilicate crystal morphology. One of them is an ellipsoid of revolution observed in Fig.10, in front and plan views. The other form is spherulitic (Figs.10 and 9). It should be noted that the spherulite diameters are close to the maximal diameters of the ellipsoids (Fig.10). The number density of spherulitic crystals is extremely low (about 2 mm^{-3}) and does not depend on the heating

rate C . This is why we suppose that these spherulitic crystals nucleated on the cooling path during glass preparation and were grown at $T_C=600^\circ\text{C}$. In other words, these are quenched-in crystals. Opposed to the quenched-in crystals, crystals formed via double stage heat treatment at nucleation and growth temperatures, or nucleated during relative low heating or cooling rates (i.e. crystals having some period of time for growth at the nucleation temperature) have a prolate ellipsoidal shape (see e.g. Fig.10). According to the experimental data shown in Fig.8, the number of athermic crystals nucleated during heating with $20^\circ\text{C}/\text{min}$ up to $T_C=600^\circ\text{C}$ is about 20 mm^{-3} . This value is lower than that estimated in ref. [60] by the DTA method (see Eq.9) by a factor of 450. Such overestimation of N_{at} results in the error of estimation $N = It_N$ and the time-lag for nucleation.

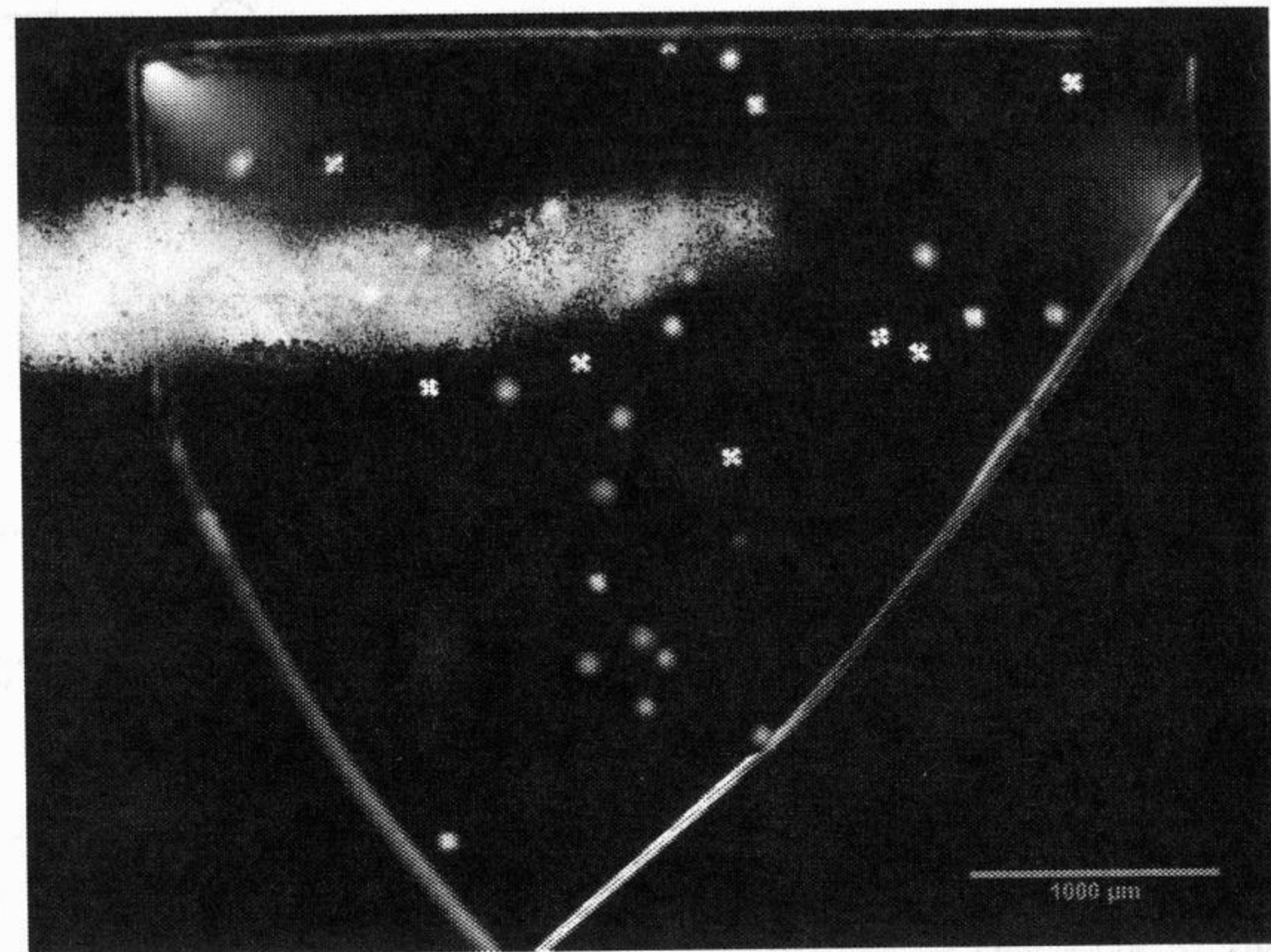


Fig.9. Micrograph (transmitted polarized light) of a Li_2S_2 glass sample treated at $T_C=600^\circ\text{C}$ during 40 min (heating rate from 20 to 600°C was about $300^\circ\text{C}/\text{min}$). The sampler is shaped as a plane-parallel plate of thickness 1.4 mm.

One should also recall that the DTA (DSC) method does not take into account surface crystallization *ipso facto* attributing the decrease in the crystallization peak area only to the preliminary volume crystallization. The following part will deal with the discrepancy between calculated and measured numbers of N_{at} , and the ratio between volume and surface crystallization.

13.2.3. Surface and volume crystallization

It is often assumed that if one uses large glass samples it is possible to neglect surface crystallization for analyses of overall crystallization kinetics. For instance, Ray and Day stated [68, 69] that internal crystallization in Li_2S_2 glass dominates over surface crystallization when the glass particle size exceeds $\sim 300\mu\text{m}$. However, it is clear that the ratio between the volume and surface crystallized fractions also depends on the intensity of the internal nucleation rates [50].

In the extreme case when the glass does not undergo internal nucleation or when it is very weak, surface crystallization dominates for all particle sizes. Thus the above characteristic size is a relative quantity depending on the time and temperature of crystallization. We carried out heat treatments of a glass powder similar to that used in the DTA run performed in ref. [60] to estimate N_{at} . The Li_2S_2 glass powder with size of

$400\text{-}500\mu\text{m}$ was heat treated in the DSC furnace at the following schedule: $20\text{-}40^\circ\text{C}$ ($5^\circ\text{C}/\text{min}$); 40°C (10 min); $40\text{-}600^\circ\text{C}$ ($20^\circ\text{C}/\text{min}$); $t_C = 20$ min; $600\text{-}20^\circ\text{C}$ ($20^\circ\text{C}/\text{min}$). Fig.11 shows photos of the glass particles subjected to the above heat treatment. It should be noted that the fine structure refers to the morphology of the crystallized surface layer. Only a few isolated crystals are observed in the particle's interior. Due to the non regular form of the particles it is difficult to quantitatively estimate the ratio between the fractions of the surface and volume crystals.

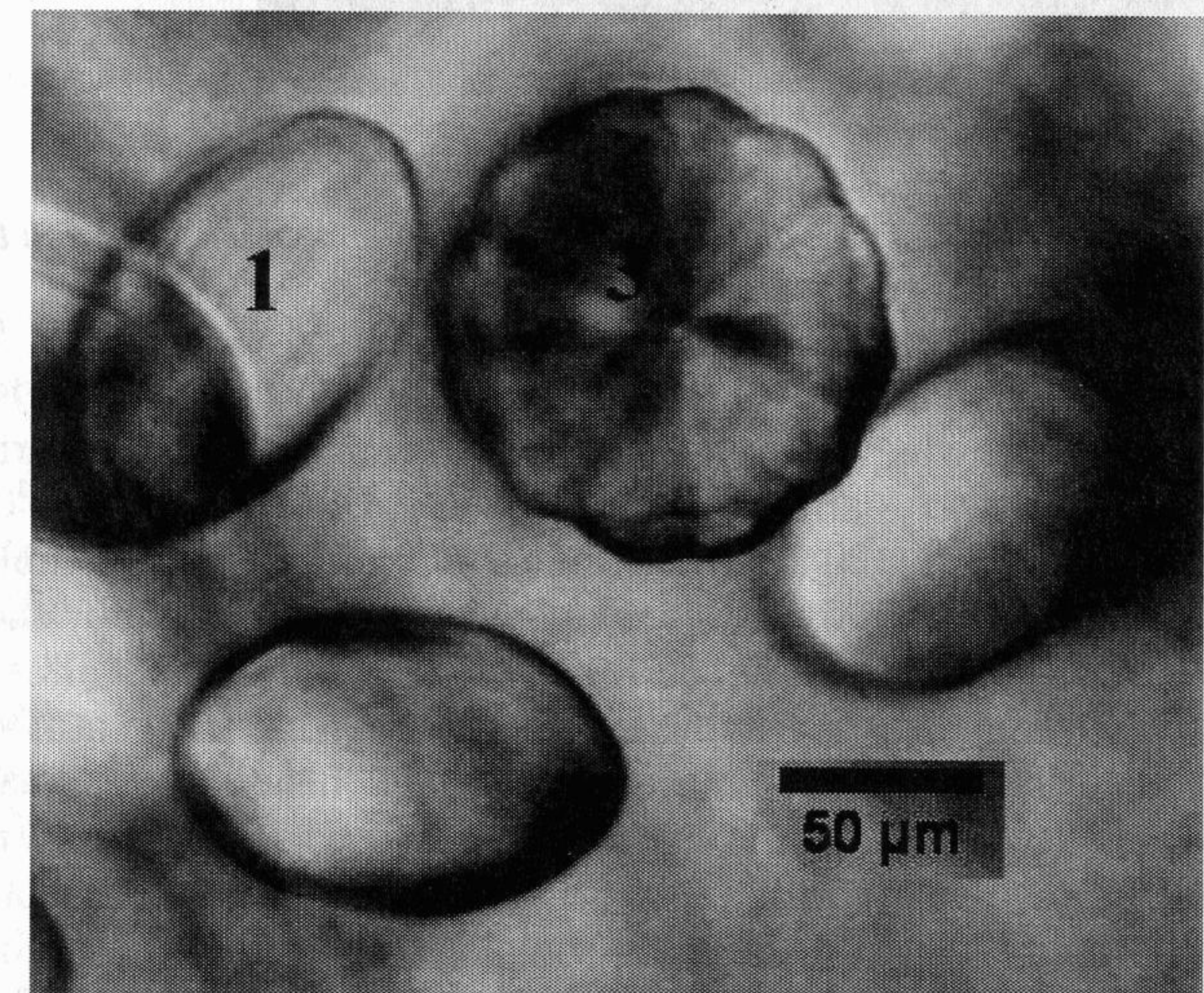
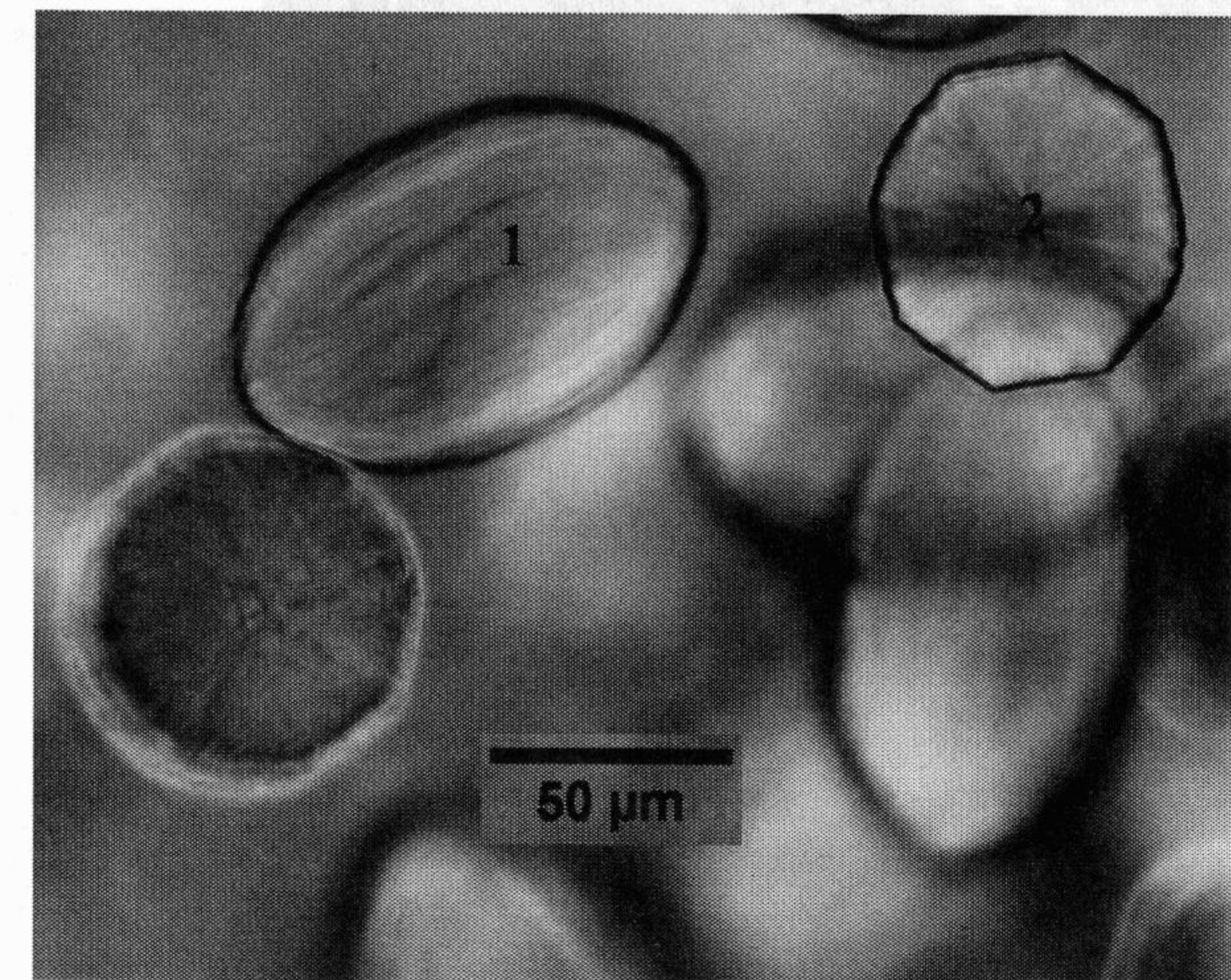


Fig.10. Micrographs (transmitted light) of lithium disilicate crystals in Li_2S_2 glass after heating with $C=10^\circ\text{C}/\text{min}$ up to $T_C=600^\circ\text{C}$ and holding at this temperature during 40 min. Ellipsoids of revolution in plan (1) and front (2) views, and spherulitic (3) lithium disilicate crystals can be observed.

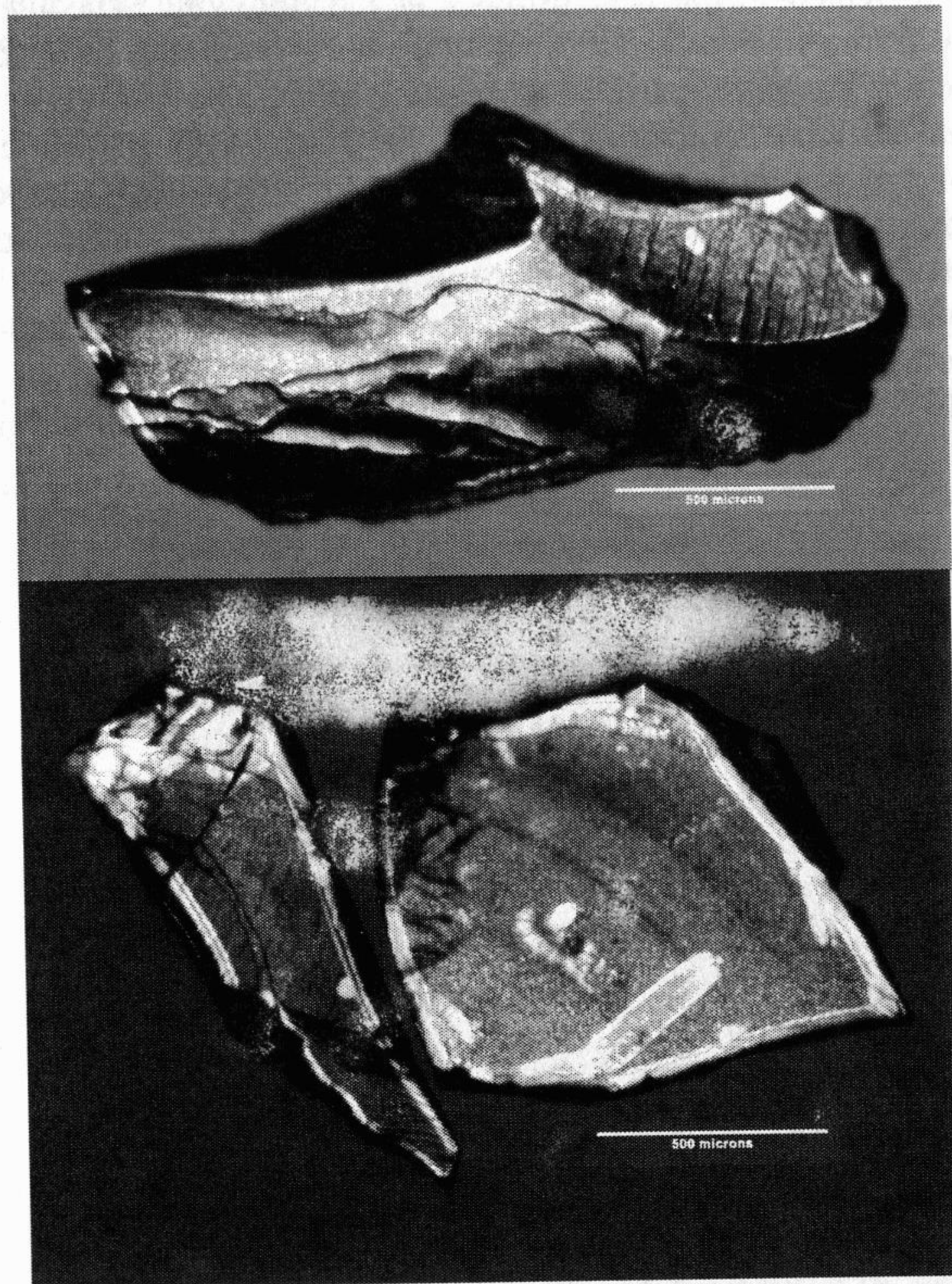


Fig.11. Photos in transmitted light of L_1S_2 glass particles after treatment performed in the DSC furnace (see text).

However, it is obvious that the volume of crystals inside the particles is lower than that of the crystals growing from the surface. For numerical comparison of fractions of surface to volume crystallization we performed DSC run ($20^\circ\text{C}-5^\circ\text{C}/\text{min} - 40^\circ\text{C} (5 \text{ min})-20^\circ\text{C}/\text{min}-620^\circ\text{C} (t_c=20 \text{ min})-20^\circ\text{C}/\text{min}-20^\circ\text{C}$) of L_1S_2 glass sampler with regular form $3.3 \times 2.8 \times 1.2 \text{ mm}^3$. Analysis of this sample via optical microscopy show that only 20% of the total crystalline phase corresponds to volume crystallization of athermic crystals. This means that neglecting surface crystallization one attributes its volume to crystals nucleated in the volume of sample and hence overestimates the number density of the latter. This effect is more pronounced when the crystal number density is low, as e.g. in the case of the athermic crystals. Of course, the contribution of volume crystallization increases when the glass sample is subjected to a preliminary nucleation heat treatment. Such the sample of L_1S_2 glass with sizes $3.4 \times 3.5 \times 1.3 \text{ mm}^3$ after DSC run including keeping at nucleation temperature ($20-40^\circ\text{C} (5^\circ\text{C}/\text{min})$; $40^\circ\text{C} (10 \text{ min})$; $40-480^\circ\text{C} (20^\circ\text{C}/\text{min})$, $t_N=30 \text{ min}$; $480-620^\circ\text{C} (20^\circ\text{C}/\text{min})$, $t_C = 10 \text{ min}$; $600-20^\circ\text{C} (20^\circ\text{C}/\text{min})$) revealed a ratio between surface and volume fractions of crystalline phase about 1:3.3.

13.2.4. Area of exothermic DTA/DSC crystallization peak

The method of Ray, Fang and Day [60] to estimate the number of nucleated crystals, briefly described previously, is based on the reasonable assumption that the area of a DTA (DSC) crystallization peak is proportional to the mass of crystallized glass. This assumption is correct if the change of sensitivity of the method with temperature is neglected. Thus one can expect that the area of the crystallization peak of the samples with the same mass or reduced per unit mass does not depend on the number density of the preliminary nucleated crystals. The temperature and time of the nucleation heat treatment have to be chosen in such way that the volume of nuclei can be neglected. This condition was fulfilled for the data presented in Fig.12.

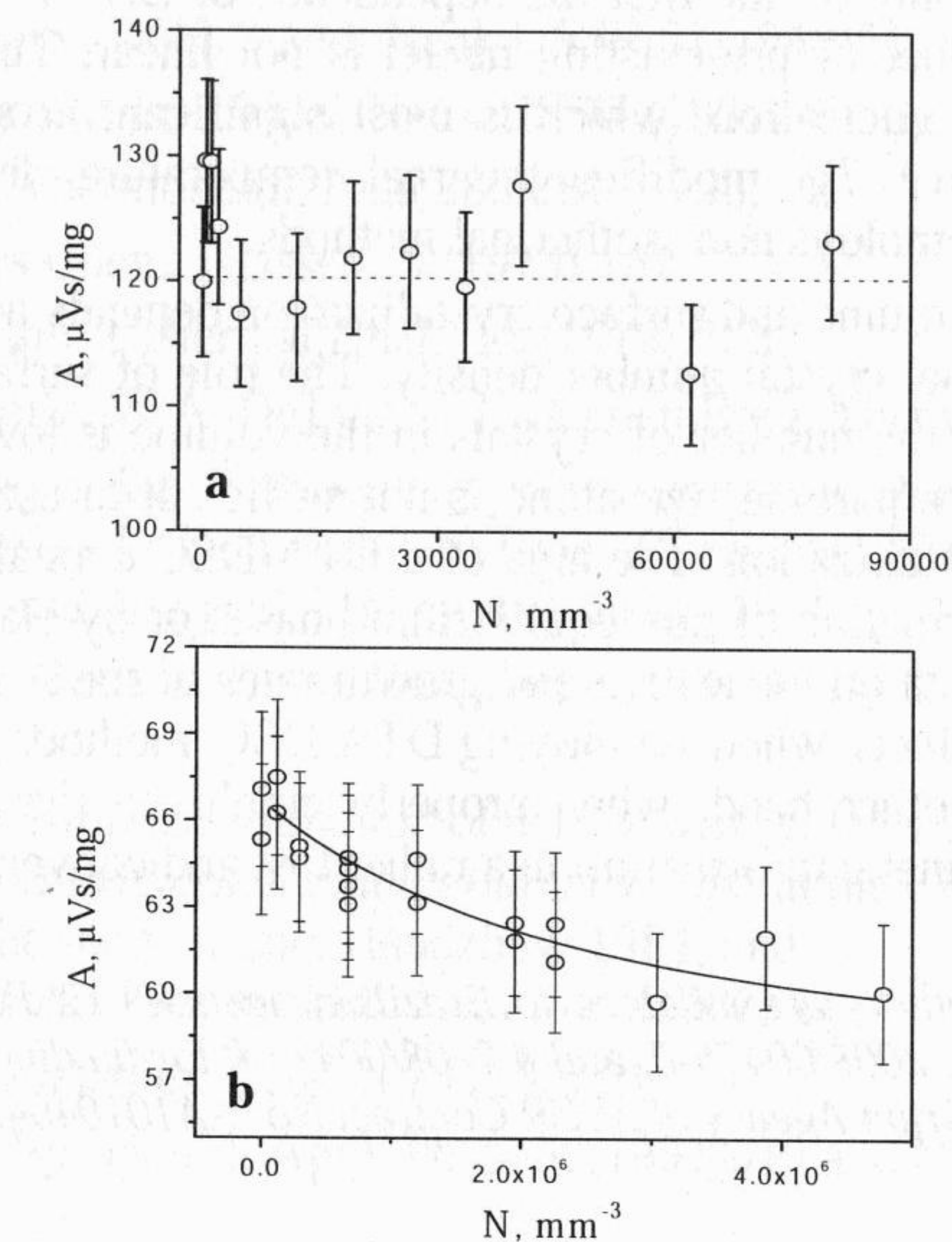


Fig.12. Area of the crystallization peak versus number of crystals for L_1S_2 (a) and $N_1C_2S_3$ (b) silicate glasses.

Indeed the variation of A with the number of crystals for L_1S_2 glass are within the error (Fig.12a), while in the case of $N_1C_2S_3$ glass (Fig.12b) one can see a weak but well defined decrease of A as the number of crystals increases. Note again that the volume of previously formed nuclei did not exceed 0.05%. The observed effect cannot be explained by the change of the sensitivity of method with temperature since an increase of N results in a decrease of T_c (see Fig.5), while the sensitivity increases with decreasing temperature. This means that the fully crystallized $N_1C_2S_3$ glass does not achieve equilibrium and the degree of non equilibrium is higher when the number of crystals is larger, i.e. the system has a more fine structure. Two reasons for the above effect seem now more probable. First of them is the structural and compositional inhomogeneity of the crystallized sample. One should recall that $\text{Na}_2\text{O} \cdot 2\text{CaO} \cdot 3\text{SiO}_2$ crystals form via nucleation of a sodium rich solid solution that during the growth process approaches the stoichiometric composition [70]. The second possibility is elastic stresses that can arise in a polycrystal. We show these dependencies of A on N only to illustrate that the obvious assumption about the proportionality of

mass of glass subjected crystallization to the area of an exothermic DSC peak is not always fulfilled.

In conclusion we can say that a robust application of the JMAK equation, in integral and derivative forms, which is frequently based on the mean values of the crystallization degree (estimated from DTA/DSC measurements) brings some doubtful results, despite the fact that a rather good discrimination of the power exponent can be achieved and can thus be related to distinguishing certain type of nucleation-growth processes, cf. Table 1. This is caused by insensitive management of averaged values determined by DTA/DSC detection of overall heat changes associated with such complex processes. Thus, it is contemplative to concentrate only on a more estranged elementary process, most wishful being the nucleation or growth separately. In this chapter we have focused only on the first the dependence of DSC/DTA crystallization peak position on the number of pre-existing nuclei is not linear. This effect together with the non-steady state nucleation (which is most significant at some temperature range below or just above T_g) modifies the real temperature dependence of the nucleation rate when one employs non-isothermal methods.

The ratio between volume and surface crystallization depends not only on sample size, but also on the internal crystal number density. The role of surface crystallization is more pronounced when the number of crystals in the volume is low, e.g. in the case of athermal crystals. Hence particle size alone is not sufficient to estimate the relative importance of surface crystallization. The area of a DTA/DSC crystallization peak can also be affected by the formation of non equilibrium phases or by elastic stresses. One needs some preliminary data on nucleation and growth rates of the studied glass to take into account all above effects when employing DTA/DSC methods to study crystallization kinetics. On the other hand, when properly employed these non isothermal methods can give useful kinetic information in a rather fast and convenient way.

Acknowledgements: The authors are indebted to Brazilian agencies CNPq # 620249/2006-4 and Fapesp # 2007/08179-9, 2008/00475-0, and # 2008/00475-0 for funding this research. The work was supported by the Grant Agency of ASCR Contract No IAA1010404.

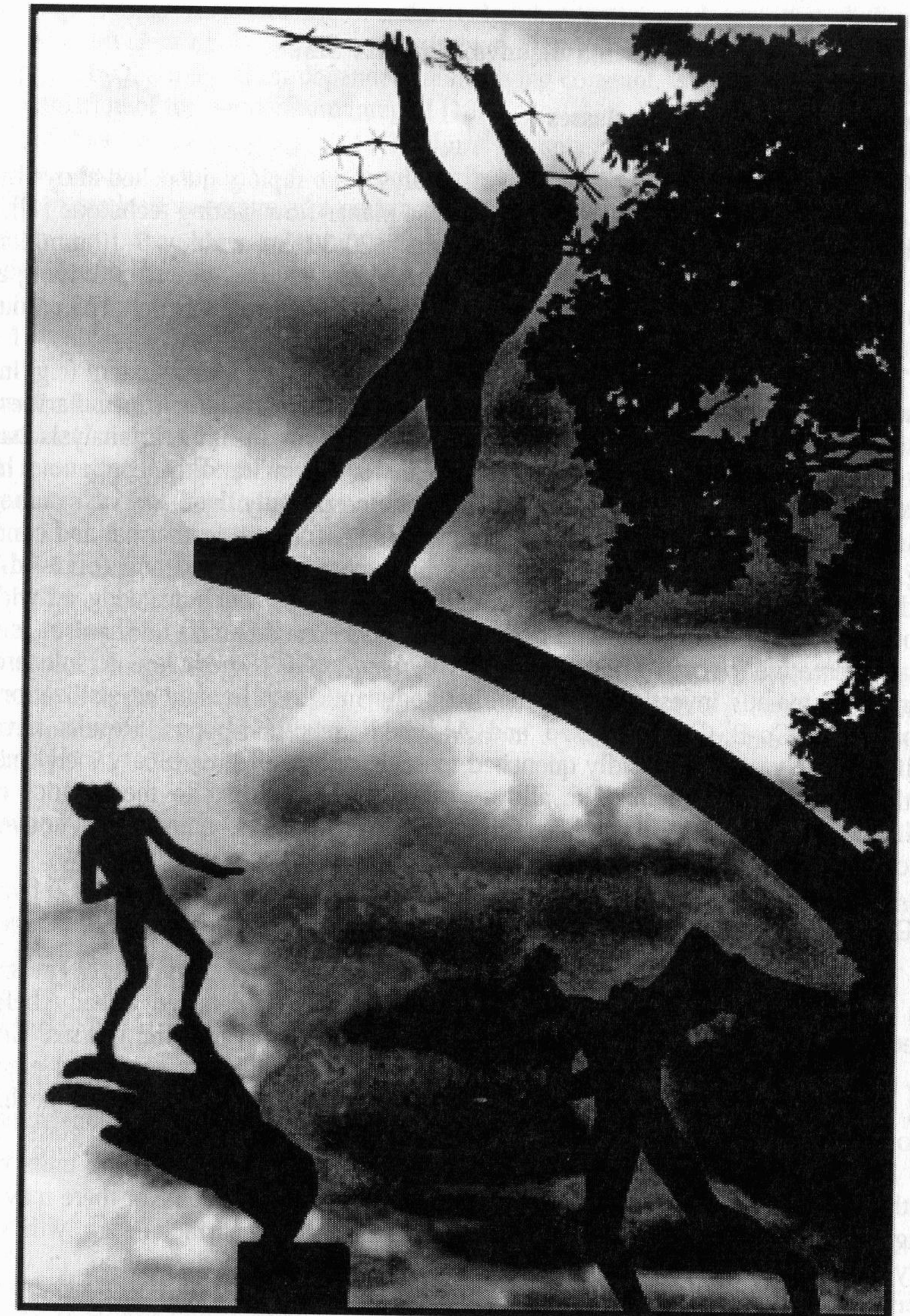
References 13

1. J. Šesták, "Thermophysical Properties of Solids: theoretical thermal analysis" Elsevier, Amsterdam 1984 and "Teoretický termičeskij analiz" Mir, Moscow 1988 (in Russian)
2. J. Šesták (ed), "Vitrification, Transformation and Crystallization of Glasses", special issue of Thermochim. Acta, Vol. 280/281, Elsevier, Amsterdam 1996
3. J. Šesták "Science of Heat and Thermophysical Studies: a generalized approach to thermal analysis" Elsevier, Amsterdam 2005
4. H.E. Kissinger, Anal. Chem. 29 (1957) 1702
5. J. Criado, A. Ortega, J. Non-cryst. Solids 87 (1986) 302
6. Y. Nishi, T. Manabe, H. Kameyana, S. Moriya, T. Katagiri, J Mater. Sci. Letters 9 (1990) 801
7. J. Llopiz, M.M. Romero, A. Juarez, Y. Laureiro, Thermochim. Acta 256 (1995)
8. L. Heireche, M. Belhadji, Chalcogenide Letters 4 (2007) 23
9. L.M. Hodge, J. Non-cryst. Solids 169 (1994) 211

10. C.T. Moynihan, S.K. Lee, M. Tatsumisago, T. Minami, Thermochim. Acta 280/281 (1996) 153
11. J. Šesták, Thermochim. Acta 3 (1971) 150
12. E.A. Marseglia, J. Non-cryst. Solids 41 (1980) 31
13. H. Yinnon, D.R. Uhlmann, J. Non-cryst. Solids 54 (1983) 253
14. S.F. Hulbert, J. Brit. Ceram. Soc. 1 (1970) 1
15. J. Šesták, J. Málek, Solid State Ionics 63/65 (1993) 245
16. J. Málek, T. Mitsuhashi, J.M. Criado, J. Mater. Res. 16 (2001) 1862
17. W.A. Johnson, R.F. Mehl, Trans. A.I.M.E. 135 (1939) 416.
18. M. Avrami, J. Chem. Phys. 7(1939)1103; 8(1940)212; 9(1941)177
19. B.V. Yerofyeyev, Dokl. Akad. Nauk USSR 52(1946)511 (in Russian)
20. A.N. Kolmogorov Izv. Akad. Nauk USSR (1937)355 (in Russian)
21. E.D. Zanotto, Thermochim. Acta 280/281 (1996) 73
22. J. Šesták, Phys Chem. Glasses 15 (1974) 137
23. D.W. Henderson, J Thermal Anal. 15 (1979) 325
24. T.J.W. DeBroijn, W.A. DeJong, P.J. van den Berg, Thermochim. Acta 45(1981)315
25. J. Šesták "Integration of nucleation-growth equation when considering non-isothermal regime" in D. Dolimore (ed) Proc. 2nd ESTAC (Europ. Symp. on Thermal Analysis), "Thermal Analysis", Heyden, London 1981, p. 115
26. A. Dobrev, I. Gutzow, Cryst. Res. Technol. 26 (1991) 863 and J Appl. Polym. Sci. 48 (1991) 473
27. J. Šesták key lecture „Distinction of crystallization kinetics determined by isothermal and non-isothermal calculation methods“ at the Chinese symposium on calorimetry and thermodynamic, Handzhow 1984; and T. Kemeny, J. Šesták, Thermochim. Acta 110 (1987) 113
28. J. Málek, Thermochim. Acta. 267 (1995) 61
29. L.C. Chen, F. Speapen, J. Appl. Phys. 69(1991)679 and Nanostruct. Mater. 11 (1992) 59
30. E. Illeková, Thermochim. Acta 280/281(1996)289 and 387(2002)47
31. H.V. Atkinson, Acta Metall. 36(1988)469
32. E. Illeková, J. Non-cryst. Sol. 287(2001)167
33. B. Idzikowski, P. Švec, M. Miglierini (eds.), "Properties and Application of Nano-crystalline Alloys" Kluwer, Dordrecht 2004
34. J. Šesták, G. Berggren, Thermochim. Acta. 3 (1971) 1
35. J.Šesták J. Thermal Anal. 36 (1990) 69
36. A.K. Burnham, J. Thermal Anal. Calor. 60 (2000) 895
37. J. A. Foreman and R. L. Blaine „Isothermal crystallization made easy: a simple SB model and modest cooling rates“ and „Isothermal crystallization using the Q Series“ in Thermal Analysis & Rheology Reports, TA Instrument Inc., New Castle 2000
38. N. Sbirrazzuoli, Y. Girault and L. Elégant, Thermochimica Acta 260 (1995) 147 and 293 (1997) 25
39. L. Koudelka, P. Mošner, P. Prokupková, J. Thermal Anal. Calor. 54 (1998) 937
40. J. Malek, Thermochim. Acta 355 (2000) 239
41. A.A. Joraid, Thermochim. Acta 436 (2005) 78

42. N. Koga, J. Šesták. Z. Strnad, Thermochim. Acta 203 (1992) 361
43. M.C. Weinberg, Thermochim. Acta 194 (1992) 93 and J. Mining Metal. (Bor, Yugoslavia) 35 (1999) 197
44. N. Koga, J. Šesták, J. Amer. Cer. Soc. 83 (2000) 1753
45. D. Clinto, A. Mercer, R.P. Miller, J. Mater. Sci. 5 (1970) 171
46. J. Málek, J. Klikorka, J. Šesták, Thermochim Acta 110 (1987) 281
47. J. Šimšová, Z. Šimša, J. Šesták, J. Non-cryst. Solids 110 (1979) 375
48. Z. Strnad, J. Šesták "Surface crystallization of $SiO_2-Al_2O_3-ZnO$ glasses" in J. Woods (ed), Proc. 8th Inter. Conf. Reactivity of Solids, "Reactions of Solids", Plenum Press, New York 1977, p. 553
49. J. Šesták. Z. Strnad "Simulation of DTA crystallization peak on basis of nucleation-growth curves determined by optical microscopy" in J. Gotz (ed), J. Proc. XI Inter. Congress on Glass, DT CVTS, Prague 1977, Vol. II, P. 249
50. N. Koga, J. Šesták, Bol. Soc. Esp. Ceram. Vidr.1 (1992) 185
51. J. Šesták, Thermochim. Acta. 98 (1986) 339
52. G. Tammann, Z. Phys. Chem. 25 (1898) 441.
53. M. Ito, T. Sakaino, T. Moriya, Bull. Tokyo Inst. Technol. 88 (1968) 124.
54. V.N. Filipovich, A.M. Kalinina, Izv. Akad. Nauk USSR, Neorgan. Mat. 4 (1968) 1532 (in Russian).
55. V.M.Fokin, E.D.Zanotto, N.S.Yuritsyn, J.W.P.Schmelzer, Review, J Non-Cryst. Solids 352 (2006) 2681.
56. A.Marotta, A.Buri, Thermochim.Acta,25 (1981) 341.
57. A.Marotta, A.Buri, F.Branda, S.Saiello "Nucleation and Crystallization of $Li_2O-2SiO_2$ Glass: A DTA Study" in J.H. Simmons, D.R. Uhlman, G.H. Beall (eds) Advances in Ceramics, Vol.4, Nucleation and Crystallization in Glasses, American Ceramic Society, Columbus, OH, 1982, pp. 146-152.
58. C.S.Ray, D.E.Day, J.Am.Ceram.Soc.,73 (1990) 439.
59. C.S.Ray, D.E.Day, J.Am.Ceram.Soc., 74 (1991) 909.
60. C.S.Ray, X.Fang, D.E.Day, J.Am.Ceram.Soc., 83 (2000) 865.
61. C.S.Ray, D.E.Day, J. Mater.Science, 37 (2002) 547.
62. P.C. Soares Jr., E.D. Zanotto, V.M. Fokin, H. Jain, J Non-Cryst. Sol. 33 (2003) 217.
63. F.C. Collins, Z. Electrochem. 59 (1955) 404
64. D. Kashchiev, Surf.Sci. 14 (1969) 209
65. Siglass data -Science Vision Version 5. www.esm-software-com/vci_glass
66. V.M. Fokin, PhD Thesis "The investigation of stationary and non-stationary crystal nucleation rate in model glasses of stoichiometric composition $Li_2O_2SiO_2$ and $2Na_2OCaO_3SiO_2$ " Institute of Silicate Chemistry of Russian Academy Sciences, 1980 (in Russian)
67. O.V. Potapov, V.M. Fokin, V.L. Ugolkov, L.Y. Suslova, V.N. Filipovich, Glass Physics and Chemistry 26 (2000) 27.
68. C.S. Ray, D.E. Day, Thermochim. Acta 280/281 (1996) 163.
69. C.S. Ray, Q. Yang, W. Huang, D.E. Day, J.Am.Ceram.Soc., 79 (1996) 3155.
70. V.M. Fokin, O.V. Potapov, E.D. Zanotto, F.M. Spiandorello, V.L.Ugolkov, B.Z. Pevzner, J Non-Cryst. Solids 331 (2003) 240.

Miles Gården, Stockholm, Sweden



Chapter 14

Metallic glasses